IL NUOVO CIMENTO **45 C** (2022) 188
DOI 10.1393/ncc/i2022-22188-2

COMMUNICATIONS: SIF Congress 2021

A digital holographic technique for studying mineral dust content in snow and ice cores

C. RAVASIO

Department of Physics, University of Milan - via Celoria, 16, I-20133 Milan, Italy

received 31 January 2022

Summary. — We propose a digital in-line holographic technique for accurate particle-by-particle characterization of airborne particles stored in meltwater samples from the cryosphere. Deriving information about particle shapes is critical to determine the intrinsic optical properties of dust, which are of great importance to increase the knowledge about aerosols and their contribution to radiative transfer through the atmosphere. To this end, digital holography has proven to be an excellent suite for distinguishing non-spherical particles, going beyond the common spherical approximation. It ensures a simultaneous measurement of particle cross-sectional area and extinction cross-section, which are important proxies in paleoclimate research and relevant to quantyifing the particle role in radiative forcing.

1. – Introduction

Aerosol consists of countless solid and liquid particles in the nanometre and micrometer size range suspended up to the stratosphere level [1]. Large deserts and arid areas entrain tiny soil particles, known as mineral dust, into the atmosphere which impacts the Earth's radiative energy balance by interacting with both solar and terrestrial radiation [2]. However, characterizing their optical properties can be challenging since they are affected by particle morphology, impurities, and coatings. Deviations from ideal spheres have an appreciable impact on the radiative forcing component from aerosols [3] and on optical depth [4]. Here we focus on the study of aerosols preserved in snow and ice cores, which have the advantage of archiving airborne particles in a clean environment protected against weathering and bioturbation. Furthermore, the high snow accumulation rate and the reliable dating of the ice cores enable sampling at a high temporal resolution. They store air bubbles, sea salts, volcanic ash, soot, dust, sands, and other pollutants, characterized by different sizes and morphology that define the deposition times and the susceptibility to long-range transport [5]. Because of the extremely low number of particles in ice core samples, an analysis on a particle-by-particle is preferable, providing a comprehensive statistical analysis and enhancing the use of the optical techniques, as

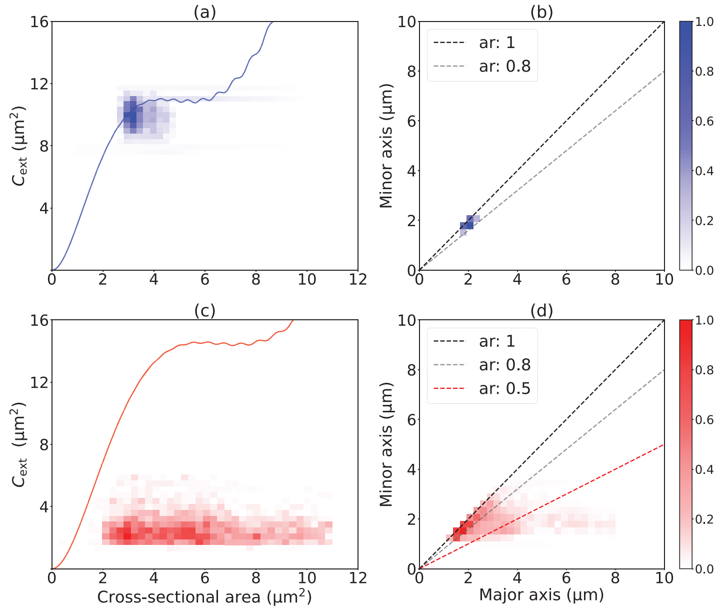

Fig. 1. – (a), (c): cross-sectional area (*csa*) according to the extinction cross-section (C_{ext}) for $2\,\mu$m diameter polystyrene (blue data) and kaolinite (red data) in water ($m = 1$) reported as a two-dimensional histogram. Counts are normalized on their maximum. The data are compared with Mie calculations for spheres with a refractive index $m = 1.19$ (blue solid line) and $m = 1.17$ (red solid line). (b), (d): the respective major and the minor axis of the *csa*. The dotted lines show where the particles lay above an aspect ratio (*ar*) of 1 (black), 0.8 (gray), and 0.5 (red).

versatile and non-invasive probes [6]. In this work, we employed a single-particle digital in-line holography (DH) technique [7], whereby we examine the scattering light from mineral dust particles content in snow, with a focus on their radiative properties and their shape.

2. – Methods

With DH, we can retrieve simultaneously the shape and several optical properties of dust stored in snow and ice cores. It is extremely simple and free from any tight alignment requirement. It consists of a collimated laser beam passing through the scattering volume, where the particles to be detected are flown. In the forward scattering direction, the (faint) fraction of diffracted light superimposes with the (almost unchanged) transmitted beam. The interference between these two fields —the *hologram*— gives rise to fringes that strictly depend on the object morphology. Once recorded, from the intensity profile of the hologram we can recover the silhouette of the mineral dust with a Huygens-Fresnel approach [8]. By simply imposing a threshold on the reconstructed intensity, we obtain the cross-sectional area (*csa*) and the cross-sectional aspect ratio (*ar*) of each particle. Moreover, digital holography allows obtaining a direct measurement of the extinction cross-section (C_{ext}) [9]. The advantage of holography with respect to traditional imaging relies on the capability of recovering images and optical information from objects within volumes much thicker than the limited depth of focus of traditional imaging or microscopy. See [10] and the references therein for additional description and applications. The experimental question we attempted to investigate is how the shape

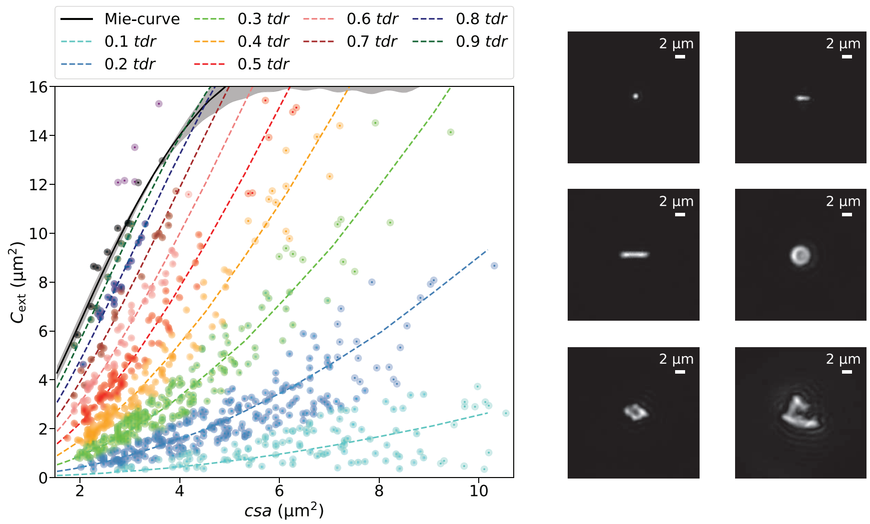

Fig. 2. – Left: cross-sectional area (csa), extinction cross-section (C_{ext}) distribution for a snowpit from the East Antarctic plateau (depth 30–150 cm). The colored lines refer to numerical oblate spheroids with $m = 1.15$ and an increasing thickness over diameter ratio (tdr) from 0.1 (turquoise line) to 1 (black line), that correspond to the Mie curve for spheres. The data points are a subset of particles whose aspect ratio approaches 1 and are coded with the same range of color. Right: some examples of particles detected in the samples, displayed from fine to coarse and aggregate particles; the white bar is set to $2\,\mu$m.

of the particles intercepting a laser beam affects their extinction cross-section.

The performance of the system has been tested with a dilute colloidal suspension of polystyrene spheres (PS, $2\,\mu$m diameter), and standard monophasic kaolinite as a benchmark for non-spherical particles. A good agreement is found with Mie calculations for the PS beads, reported with a blue continuous line in fig. 1(a). On the contrary, comparing kaolinite with a distribution of spheres (fig. 1(c), red line) does not match the actual C_{ext} of the oblate particles, since these clearly have lower extinction, even for isometric csa. This is further evidenced in fig. 1(b), (d), where the major and minor axes of the csa are shown, obtained as the height and width of a (possibly rotated) bounding rectangle around each particle. The PS distribution lays between an ar value of 0.8 and 1 (gray and black dashed lines), while the kaolinite distribution shows a consistent number of particles with ar less than 0.5 (red dashed line), as expected by non-spherical particles. Anyway, despite the fact that oblate particles are located lower in the (csa, C_{ext}) plane, we found a number of particles with ar close to unity.

3. – Results

In the following, we report an example of DH application by studying meltwater samples from a snowpit collected along the East Antarctic International Ice Sheet Traverse across the East Antarctic plateau. Here, we found broad distributions both for C_{ext} (1–20 μm^2) and csa (1–10 μm^2) values [10]. Some examples of the outputs of the technique are shown in fig. 2 (right), which reveals a variety of particle morphologies, from isometric and needle-like (the most common) to coarse and aggregates particles (occasional). To compare our data to the spherical model, we take only the particles with isometric *csa*. However, in fig. 2 (left) we can see that there is not a straightforward correlation between C_{ext} and *csa*, which is a consequence of the presence of flat oblate particles, whose extinction is lower than it is for spheres, as we showed also in fig. 1(c). By comparing the C_{ext} of simulated oblate spheroids with an incremental thickness over diameter ratio (*tdr*) to our data, we can distinguish our particles depending on their thickness. Small *tdr* correspond to flat particles while, as *tdr* increases, the shape tends to a sphere. The analysis reveals a prevalence of *tdr* values between 0.15 and 0.4. Finally, having the three dimensions of the particles, we can give an estimate of the volume. We find that the C_{ext} of the particles would have been overestimated by a factor up to ~ 3 for flat shape in comparison to the spherical approximation.

4. – Discussion

This work is a brief overview of the capability of the DH technique to characterize dilute and polydisperse micrometric dust particles, by reporting a suite of validation measurements with calibrated particles and by giving an example of a liquid sample from the East Antarctic plateau. We provide information about the morphological and optical properties with a single-particle approach. Our focus is on the effect their shape has on their scattering properties, which translates into a contribution to the Earth's radiative transfer. The results and the numerical simulations show the prevalence of non-spherical particles in the sample accordingly. The data exhibits a broad extinction distribution, depending on their thickness. A quantitative analysis has been performed, whereby we differentiated particles of comparable size. A critical aspect that arises from the experimental data is the importance of a multi-parametric characterization to obtain reliable particle information. We found that the extinction cross-section of spherical particles (*tdr* $\sim$ 0.8–1) is up to 3 times that of flat particles (*tdr* $\sim$ 0.1–0.2). With simultaneous measurement of the 1) extinction cross-section and 2) cross-sectional area, we can overcome this overestimation.

* * *

The author acknowledges Dr. Barbara Delmonte (EuroCold Laboratory, University of Milan-Bicocca) for the snow samples; Prof. Marco A. C. Potenza (University of Milan), and his colleagues for the general overview of the work.

REFERENCES

[1] Seinfeld John H. and Pandis Spyros N., *Atmospheric Chemistry and Physics: From Air Pollution to Climate Change* (John Wiley & Sons) 2016.
[2] Stocker T. *et al.*, *Climate Change 2013: The Physical Science Basis* (Cambridge University Press) 2013.
[3] Dubovik *et al.*, *J. Geophys. Res. Atmos.*, **111** (2006) D11.
[4] Potenza M. A. C. *et al.*, *Sci. Rep.*, **6** (2016) 1.
[5] Delmonte B. *et al.*, *Clim. Dyn.*, **23** (2004) 3.
[6] Cremonesi L. *et al.*, *Aerosol Sci. Technol.*, **54** (2020) 4.
[7] Gabor Dennis, *Nature*, **161** (1948) 777.
[8] Latychevskaia Tatiana and Fink Hans-Werner, *Appl. Opt.*, **54** (2015) 9.
[9] Berg Matthew J. *et al.*, *Opt. Lett.*, **39** (2014) 13.
[10] Ravasio C., Cremonesi L. *et al.*, *ACS Earth Space Chem.*, **5** (2021) 10.